Liem et al., http://www.jcb.org/cgi/content/full/jcb.201110049/DC1

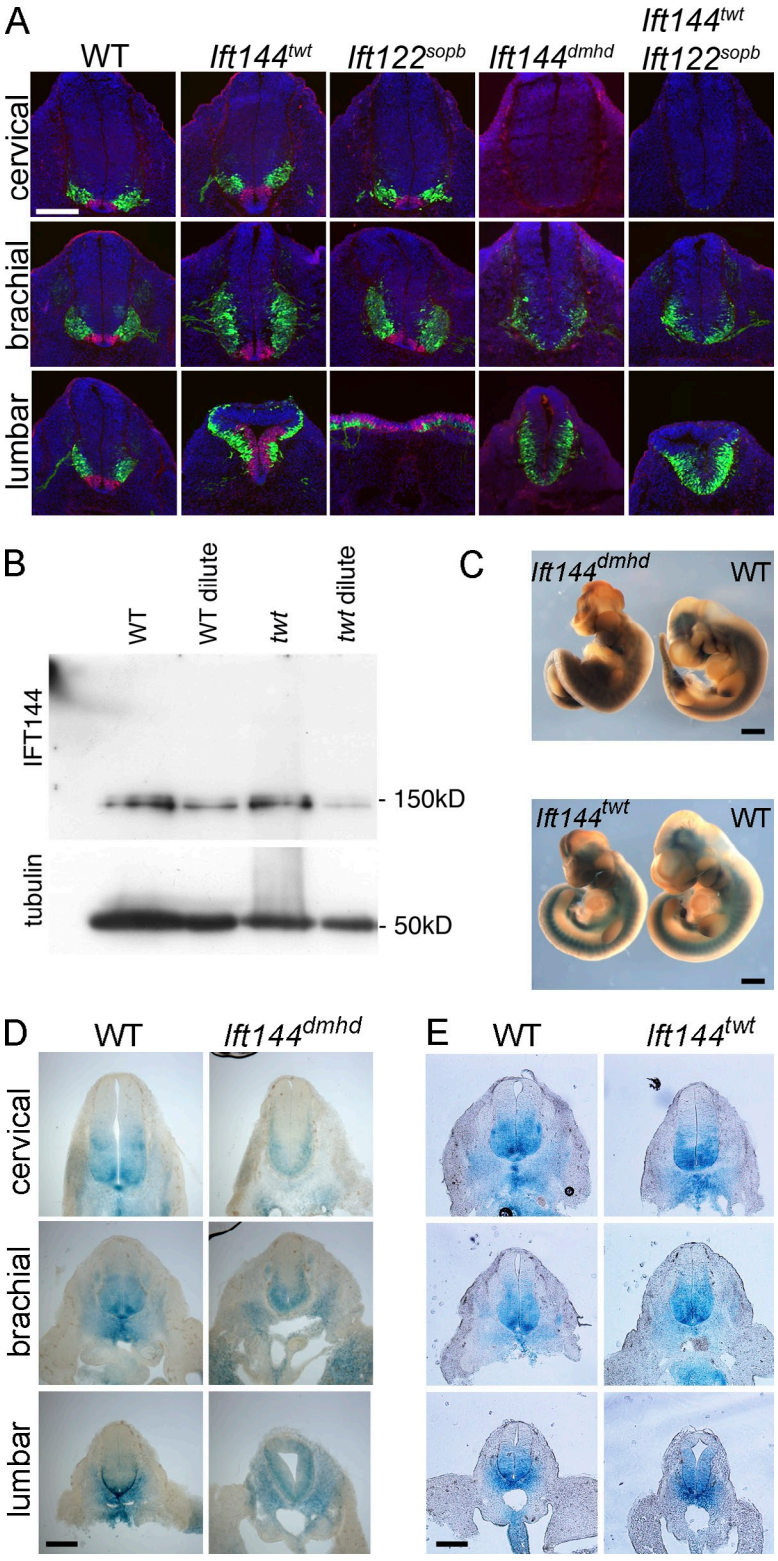

Figure S1. **Molecular and phenotypic characterization of the *Ift144*^{twt} and *Ift144*^{dmhd} mutants.** (A) Nkx2.2 expression in the lumbar neural tube. The V3 progenitor marker Nkx2.2 (red) is expanded dorsally in E10.5 *Ift144*^{twt} and *Ift122*^{sopb} neural tube, especially at caudal levels. Nkx2.2+ cells are absent in *Ift144*^{dmhd} embryos and in *Ift144*^{twt} *Ift122*^{sopb} double mutants. Motor neurons are marked with HB9-GFP (green). WT, wild type. Bar, 200 µm. (B) The *Ift144*^{twt} mutation does not affect the amount of the protein made. Protein extracts from E18 brains were prepared and loaded undiluted or threefold diluted on the gel, and the gel was blotted for IFT144 protein. The blots were reprobed for α-tubulin as a loading control. The amount of IFT144 protein present in *Ift144*^{twt} homozygotes relative to the loading control is similar to the amount present in wild type. The abundance of IFT144 at earlier embryonic stages was too low for detection by the antibody, precluding analysis of the protein in *Ift144*^{dmhd} embryos. (C) *Ptch1-lacZ* expression in E10.5 *Ift144* mutant embryos. *Ptch1-lacZ* expression is decreased in the anterior spinal cord levels in *Ift144*^{dmhd} embryos but is increased in caudal regions, notably in mesoderm in the trunk. *Ift144*^{twt} embryos have mildly elevated *Ptch1-lacZ* in the neural tube. Bars, 1 mm. (D) Sections show that the high level of *Ptch1-lacZ* expression in the ventral region of the cervical and brachial neural tube is reduced in *Ift144*^{dmhd} embryos; at the same time, *Ptch1-lacZ* is expressed ectopically in the mesenchyme and caudal neural tube of the mutants. (E) *Ptch1-lacZ* is expressed ectopically in the dorsal neural tube of *Ift144*^{twt} embryos, especially at lumbar levels; expression in mesenchymal cells is also elevated. There was a striking expansion of the expression domain of *Ptch1-lacZ* in the flank and in the limb bud *Ift144*^{dmhd} embryos (D), particularly at caudal levels, and a milder elevation in *Ift144*^{twt} embryos (E; also see Ashe et al., 2012). Thus, the effects of the *Ift144* mutations on Shh signaling were both position and tissue dependent.

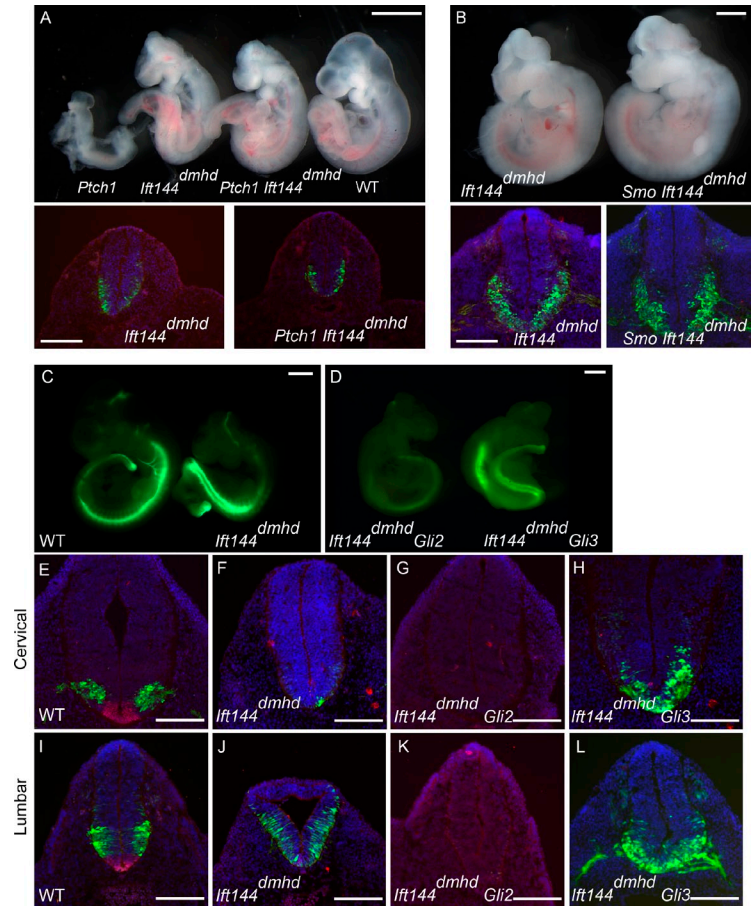

Figure S2. ***Ift144* acts downstream of *Ptch1* and *Smo* and upstream of *Gli2* and *Gli3*.** (A) Ptch1, the Shh receptor, is a negative regulator of the pathway; *Ptch1* mutants arrest at E9.0 with a strong gain-of-function Shh phenotype. *Ift144*^{dmhd} *Ptch1* embryos survive to E10, whereas *Ptch1* embryos arrest at E9.0. The double mutants have the same morphology as *Ift144*^{dmhd} embryos. Brachial sections of E9.5 *Ift144*^{dmhd} and *Ift144*^{dmhd} *Ptch1* embryos show the same ventral domain of expression of HB9-GFP in the neural tube and fail to express Nkx2.2 (red), indicating that activation of the Shh pathway caused by loss of *Ptch1* depends on IFT144 function. WT, wild type. (B) *Smo* mutant embryos arrest at E9.0 and lack all Shh signaling (Caspary et al., 2002). The external morphology of E10.5 *Ift144*^{dmhd} *Smo* double mutants is indistinguishable from that of *Ift144*^{dmhd} single-mutant embryos, and the double and single mutants show the same ventral expression of HB9-GFP and fail to express FoxA2 (red), indicating that IFT144 acts downstream of Smo, like other IFT proteins (Huangfu and Anderson, 2005). (A and B) Bars: (top) 1 mm; (bottom) 200 µm. (C–L) The pattern of motor neurons in *Ift144*^{dmhd} depends on Gli2 and Gli3. The Gli2 and Gli3 transcription factors implement Shh activity in the neural tube (Bai et al., 2004); Gli2 acts primarily to activate target gene expression, and Gli3 acts primarily to repress target gene activity in the absence of ligand. (C and D)Whole-mount E10.5 embryos expressing HB9-GFP (green). In contrast to *Ift144*^{dmhd} (C), where HB9-GFP is strongly expressed in the caudal neural tube but is absent from the rostral neural tube, HB9-GFP is not expressed in *Ift144*^{dmhd} *Gli2* double mutants and is expressed both rostrally and caudally in *Ift144*^{dmhd} *Gli3* embryos (D). Cross-sections of E10.5 embryos at cervical (E–H) and lumbar (I–L) levels are marked by the expression of HB9-GFP for motor neurons and FoxA2 for the floor plate. *Ift144*^{dmhd} *Gli2* double-mutant embryos (G and K) lack motor neurons at all levels, in contrast to the expanded motor neuron domain in the lumbar region of *Ift144*^{dmhd} single mutants (J). Thus, the specification of ectopic motor neurons in the caudal neural tube of *Ift144*^{dmhd} mutants is a result of inappropriate activation of Gli2. *Ift144*^{dmhd} *Gli3* double mutants specified motor neurons in both the cervical and lumbar neural tube (H and L), indicating that the absence of motor neurons in the *Ift144*^{dmhd} rostral neural tube is a result of Gli3-mediated repression. Because removal of either Gli2 or Gli3 eliminates the rostrocaudal differences in patterning seen in *Ift144*^{dmhd}, those differences must reflect the different roles of Gli2 and Gli3 in the response to Shh along the rostrocaudal axis. Bars: (C and D) 1 mm; (E–L) 200 µm.

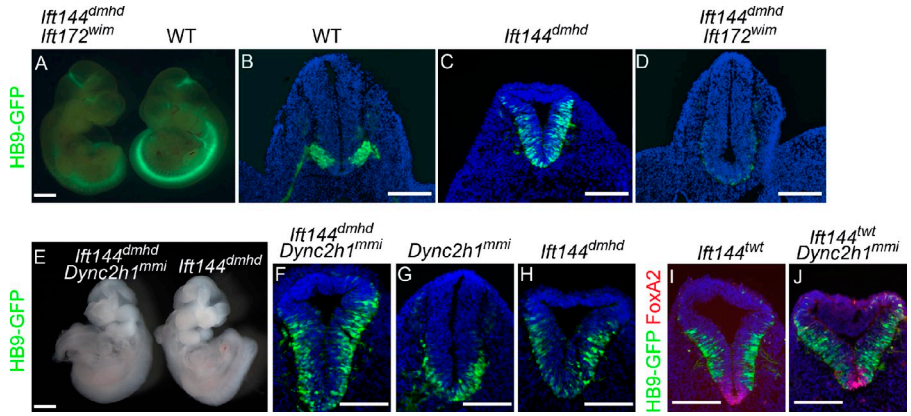

Figure S3. ***Ift144*^{dmhd} neural patterning phenotype depends on cilia but is independent of Dync2h1.** (A) HB9-GFP is not expressed in the *Ift144*^{dmhd} *Ift172*^{wim} double-mutant embryo compared with a wild-type (WT) littermate at E10.5. (B–D) Sections through the lumbar neural tube of HB9-GFP–expressing embryos. In contrast to wild type (B) and *Ift144*^{dmhd} (C), *Ift144*^{dmhd} *Ift172*^{wim} double mutants (D) do not generate HB9-GFP–expressing motor neurons. (E) E10.5 *Ift144*^{dmhd} *Dync2h1*^{mmi} double-mutant embryos resemble *Ift144*^{dmhd} embryos. (F–H) The lumbar region of *Ift144*^{dmhd} *Dync2h1*^{mmi} double-mutant embryos has an expanded motor neuron domain, similar to *Ift144*^{dmhd} mutants. (I–J) *Ift144*^{twt} *Dync2h1*^{mmi} mutants have expanded motor neurons and FoxA2^{+} floor plate cells at lumbar regions, as in *Ift144*^{twt} single mutants. Bars, 200 µm.

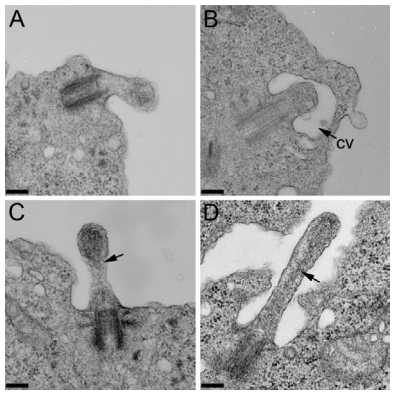

Figure S4. **The range of structural defects in *Ift144*^{dmhd} neural cilia, as seen by TEM.** (A) Most *Ift144*^{dmhd} neuroepithelial cell cilia are short, and most lack axonemal microtubules. (B) Some mutant cilia project into a ciliary vesicle (CV) that has not fused with the plasma membrane. (C and D) A few microtubules (arrows) are visible in longer *Ift144*^{dmhd} cilia. (D) Occasional cilia of wild-type length can be found. Bars, 200 nm.

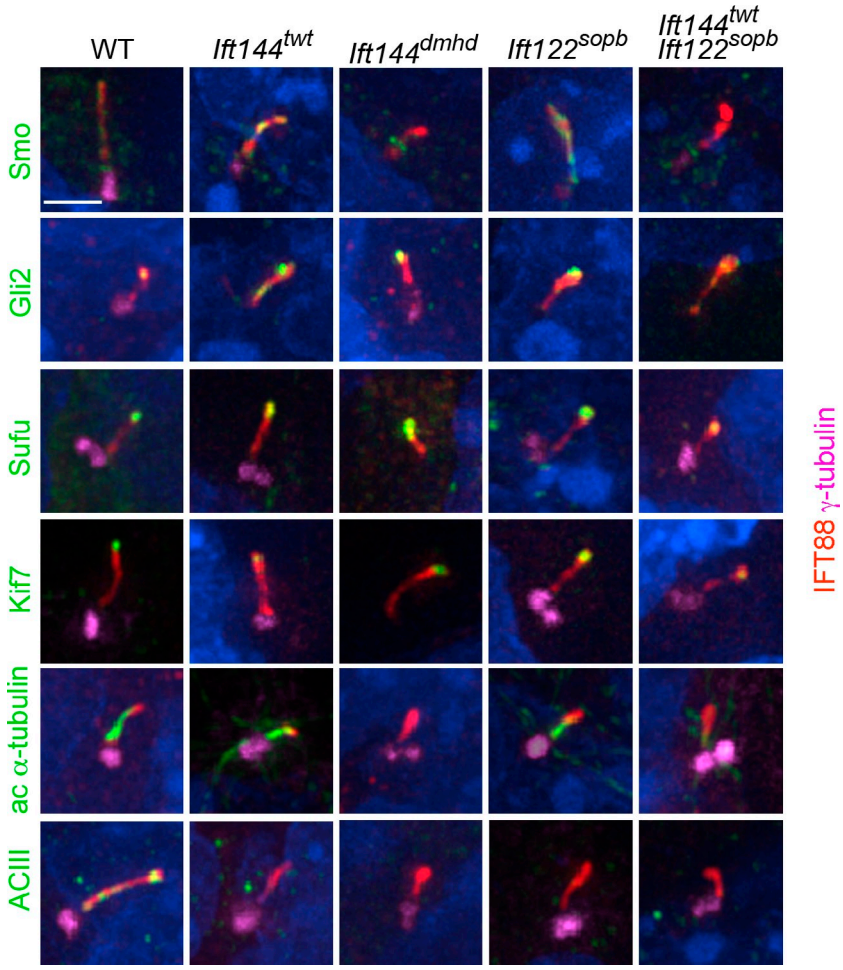

Figure S5. **Localization of Shh pathway and ciliary proteins in IFT-A mutant embryonic mesenchymal cells.** The distribution of ciliary proteins in mesenchymal cells in the embryo adjacent to the notochord was assayed; note that neural cilia are too tightly packed to allow analysis of localization of proteins to individual cilia. The basal body is stained for γ-tubulin; the axoneme is stained with IFT88. Smo is present in wild-type (WT), *Ift144*^{twt}, and *IFT122*^{sopb} mesenchymal cilia but does not enter the cilia of *Ift144*^{dmhd} and *Ift144*^{twt} *Ift122*^{sopb} double mutants. Gli2, Sufu, and Kif7 are localized to cilia tips both in wild-type and IFT-A mutant mesenchymal cilia. The ciliary marker acetylated (ac) α-tubulin was detected in wild-type, *Ift144*^{twt}, and *Ift122*^{sopb} embryonic cilia but not in cilia of *Ift144*^{dmhd} and *Ift144*^{twt} *Ift122*^{sopb} double-mutant embryos. ACIII was present in wild-type mesenchymal cell cilia but was absent or less intense in the cilia of mesenchymal cells in IFT-A mutant embryos. The quantitation for cilia localization of the Shh pathway protein in mesenchymal cilia is shown in Table S2. Bar, 2 µm.

Table S1. **Cilia dimensions in wild type and mutants**

Genotype	Cilia length	Cilia width	*n*
	nm	*nm*	
Wild type	804 ± 48	151 ± 5.2	20
Ift144^{dmhd}	466 ± 34	244 ± 10	24
Ift144^{twt}	770 ± 30	192 ± 9	11
Ift144$^{twt/dmhd}$	597 ± 33	215 ± 9	13
Ift122^{sopb}	701 ± 25	248 ± 8	23
Ift144^{twt} *Ift122*^{sopb}	456 ± 25	278 ± 8	27
Dynch1^{mmi}	711 ± 43	276 ± 11	8
Ift144^{twt} *Dynch1*^{mmi}	750 ± 40	245 ± 9	16

The dimensions of E10.5 neural tube cilia, as determined by scanning electron microscopy, are shown.

Table S2. **Cilia localization of Shh pathway proteins in embryonic mesenchymal cells**

Genotype	Kif7	Sufu	Gli2	Smo	ACIII
	%	%	%	%	%
Wild type	89 (66)	93 (57)	95 (57)	77 (109)	76 (17)
Ift144^{dmhd}	92 (12)	100 (18)	97.5 (40)	7.4 (54)	0 (26)
Ift144^{twt}	92 (13)	100 (20)	100 (46)	88 (51)	48 (10)
Ift122^{sopb}	94 (17)	94 (16)	91 (23)	81 (42)	16 (12)
Ift144^{twt} *Ift122*^{sopb}	81 (33)	100 (40)	83 (24)	14 (71)	20 (15)

The percentage of cilia (marked by IFT88) showing detectable enrichment of proteins in cilia of mesenchymal cells in wild-type and mutant E10.5 embryos (as in Fig. 8) is indicated; the number of cilia examined is shown in parentheses. For ACIII, both the number of positive cilia and the intensity of staining in ACIII+ cilia were reduced in the mutants. The intensity of the ACIII signal in *Ift144*^{twt} was 30% of that in wild type, 20% of wild type in *Ift122*^{sopb}, and 3% of wild type in *Ift144*^{twt} *Ift122*^{sopb}.